# Electrically driven singlet-triplet transition in triangulene spin-1 chains

Gabriel Martínez-Carracedo,[1,2] László Oroszlány,[3,4] Amador García-Fuente,[1,2] László Szunyogh ⓘ,[5,6] and Jaime Ferrer[1,2]

[1]*Departamento de Física, Universidad de Oviedo, 33007 Oviedo, Spain*

[2]*Centro de Investigación en Nanomateriales y Nanotecnología, Universidad de Oviedo–CSIC, 33940 El Entrego, Spain*

[3]*Department of Physics of Complex Systems, Eötvös Loránd University, 1117 Budapest, Hungary*

[4]*MTA-BME Lendület Topology and Correlation Research Group, Budapest University of Technology and Economics,*
*Műegyetem rkp. 3., H-1111 Budapest, Hungary*

[5]*Department of Theoretical Physics, Institute of Physics, Budapest University of Technology and Economics,*
*Műegyetem rkp. 3., H-1111 Budapest, Hungary*

[6]*ELKH-BME Condensed Matter Research Group, Budapest University of Technology and Economics,*
*Műegyetem rkp. 3., H-1111 Budapest, Hungary*

Recently, graphene triangulene chains have been synthesized, and their magnetic response has been analyzed by scanning tunneling microscopy methods by Mishra *et al.* [Nature (London) **598**, 287 (2021)]. Motivated by this study, we determine the exchange bilinear and biquadratic constants of the triangulene chains by calculating two-spin rotations in the spirit of the magnetic force theorem. We then analyze open-ended, odd-numbered chains, whose edge states pair up forming a triplet ground state. We propose three experimental approaches that enable us to trigger and control a singlet-triplet spin transition. Two of these methods are based on applying a mechanical distortion to the chain. We finally show that the transition can be controlled efficiently by the application of an electric field.

## I. INTRODUCTION

Simple spin models have played a key role in the formulation and comprehension of the basic principles of magnetism and statistical mechanics since the early days of quantum theory [1,2]. The interest in these models and in the systems realizing them persists today due to their connection to many topological properties of matter [3,4], as well as their potential to become the building blocks of viable and robust quantum computers [5,6]. Infinite quantum antiferromagnetic (AFM) spin-1 chains have a singlet ground state and a gap in their excitation spectrum [3]. This is because each atomic spin fractionalizes into two spin-$\frac{1}{2}$ states, and each spin-$\frac{1}{2}$ state entangles with another one at a neighbor site forming a singlet. The spin-1 chain therefore decomposes into a set of singlet dimers [7,8]. Further numerical work [8–10] on the open-ended bilinear-biquadratic (BLBQ) nearest-neighbor model

$$\hat{H}_{\mathrm{BLBQ}} = J \sum_{i=1}^{N-1} [\hat{\mathbf{S}}_i \cdot \hat{\mathbf{S}}_{i+1} + \beta(\hat{\mathbf{S}}_i \cdot \hat{\mathbf{S}}_{i+1})^2] \qquad (1)$$

has shown that a spin-$\frac{1}{2}$ edge excitation appears at each of the two ends, whose energy lies inside the Haldane gap. These edge states entangle into a singlet and a triplet, whereby the singlet (triplet) is the ground state for even (odd) $N$ chains, and the singlet-triplet energy splitting $\Delta E_{\mathrm{ST}} = E(S = 1) - E(S = 0)$ decays exponentially with the chain length.

Theoretical and experimental works have explored already the potential of the singlet-triplet transition of these edge modes for storage and manipulation of quantum information

[5,11–13]. However, efforts to realize unequivocally quantum spin-1 chains have been hindered by a variety of factors, among which the magnetic anisotropy arising from the spin-orbit interaction is possibly the most relevant one. Recently, graphene triangulenes (GTs) have been synthesized as single molecules [14,15], or forming chains [16], where due to Lieb's theorem [17,18] each triangulene block is characterized by a robust spin-1 magnetic moment. Because the constituent carbon atoms have a negligible spin-orbit interaction, GT chains are faithful realizations of the open-ended spin-1 quantum AFM chain model embodied in Eq. (1).

We propose in this paper three experimental approaches to trigger and control a singlet-triplet transition for odd-numbered AFM spin-1 GT chains. The proposals are based on the experimental bottom-up approach of Mishra *et al.* [16] that leads to chains of many different lengths and shapes. Specifically, horseshoe-shaped chains of different lengths were synthesized; see the example sketched in Fig. 1(a). Because increasing the length $N$ of the chain increases its ductility, the two ends of the chain can be brought in close proximity, which in turn introduces an exchange coupling $J_{1N}$ between the two magnetic degrees of freedom localized at the edges. Since the ground state of odd-numbered chains is a triplet, while that of a cyclic chain is a singlet, there must be a critical $J_{1N}^c$ separating the two ground states, as depicted in Fig. 1(b).

The experimental feasibility of the proposals is ensured by the ability to manipulate and measure spectroscopically graphene nanostructures by scanning tunneling microscopy (STM) methods [15,16,19,20]. We establish first the requirements for a triplet-singlet level crossing via exact
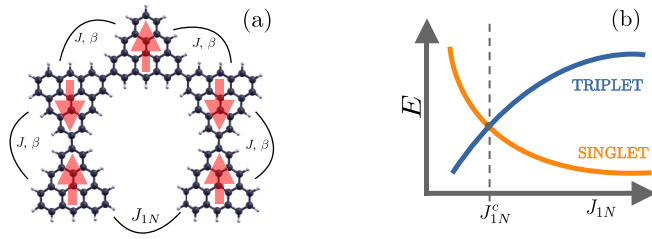
FIG. 1. (a) Sketch of a horseshoelike $N = 5$ GT chain, where the spins at each triangulene pair are coupled by the same exchange constants $J$ and $\beta$, and where the two end GT spins are coupled by a smaller exchange constant $J_{1N}$. (b) A singlet-triplet crossing occurs at a finite value of $J_{1N}/J$ smaller than 1.

diagonalization. We then use a first-principles approach to map GT chains to one-dimensional spin-1 Heisenberg chains and extract the corresponding exchange constants. The main prediction of our study is that the critical interedge constant $J_{1N}^c$ can be reached by experimentally feasible mechanisms, especially, by the application of an external electric field.

## II. METHOD

### A. Exact diagonalization

We compute here the energy spectrum of the Hamiltonian

$$\hat{H} = \hat{H}_{\text{BLBQ}} + J_{1N}\hat{\mathbf{S}}_N \cdot \hat{\mathbf{S}}_1 \qquad (2)$$

for odd-$N$ chains from $N = 3$ to $N = 15$. Our calculations for $J_{1N} = 0$ show that a singlet edge state and a triplet edge state lie inside the Haldane gap as expected, the triplet being the ground state.

We search for the critical value $J_{1N}^c$ of the exchange constant that renders a fourfold degenerate ground state. Figure 2(a) shows that $J_{1N}^c/J$ decays exponentially with $N$. Figure 2(b) demonstrates that larger values of $\beta$ facilitate reaching the critical $J_{1N}^c$. All in all, we find that the singlet-triplet crossing happens at reasonably small values of $J_{1N}/J \sim 0.01$–$0.2$ if $N$ is larger than 7 and for values of the biquadratic parameter $\beta$ relevant for the GT chains extracted both experimentally [16] and in the first-principles mapping presented below.

The exponential decay of $J_{1N}^c$ with $N$ means that the singlet-triplet energy splitting $\Delta E_{\text{ST}}$ also decays with $N$. We
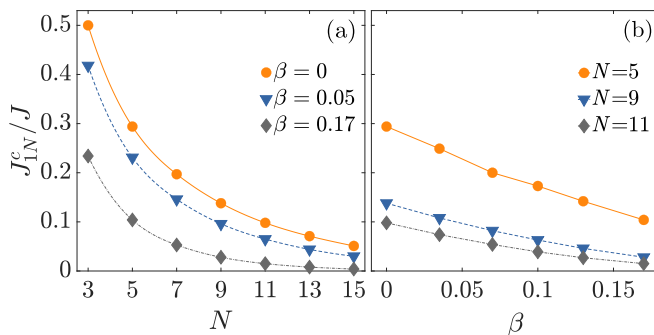


FIG. 2. (a) $J_{1N}^c/J$ as a function of $N$ for several values of $\beta$. (b) $J_{1N}^c/J$ as a function of $\beta$ for chains having different lengths.

find that values of $\Delta E_{\text{ST}}$ larger than about 1 meV require exchange constants $J_{1N}/J > 0.1$ (calculations with many values of $N$ are shown in the Supplemental Material [21]). We show in the next section that the energy scale of the singlet-triplet splitting can be tuned on the order of a few meV, so that it should be easily resolved experimentally using spectroscopic methods.

### B. *Ab initio* simulations of GT chains

We have carried out density functional theory (DFT) simulations of GT chains having an odd number of GTs, as shown in Fig. 1(a). Each GT contains 22 carbon atoms and has zigzag edges where each edge carbon atom has been passivated with hydrogen. We have used the DFT package SIESTA [22], with the generalized gradient approximation [23]. We have used established pseudopotentials for carbon and hydrogen and strict accuracy tolerances such as a real-space grid cutoff of 500 Ry. We have first confirmed that the total spin of a single isolated GT is $s = S/\hbar = 1$ via a Mulliken analysis. We have then simulated odd-numbered chains possessing AFM spin alignment. We have found that the total charge and spin of each GT in the chain are the same as those of an isolated GT up to four to five decimal digits. We therefore conclude that charge fluctuations among GTs are frozen and that the low-energy sector of the Hilbert space of each GT corresponds to that of a quantum spin-1 degree of freedom.

### C. Mapping to the BLBQ model

We can extract the bilinear ($J$) and biquadratic ($\beta$) constants that couple the spin-1 degrees associated with GTs, by making use of the fact that in the absence of spin-orbit coupling any collinear state is either stable or metastable. The energy cost of infinitesimal rotations of the spins from their collinear reference states at two different GTs ($n \neq m$) in a chain can be expanded to second order as [21]

$$\delta E_{nm}^{(2)} = D_{nm}^{(2)}\delta\mathbf{S}_n \cdot \delta\mathbf{S}_m, \qquad (3)$$

where

$$D_{nm}^{(2)} = J_{nm}(1 + 2\beta_{nm}(\mathbf{S}_n \cdot \mathbf{S}_m)). \qquad (4)$$

We apply the generalization of the Liechtenstein-Katsnelson-Antropov-Gubanov (LKAG) formula to the case of a nonorthonormal basis set [24] to determine $D_{nm}^{(2)}$, in the spirit of the magnetic force theorem [25–27]. We compute $D_{nm}^{(2)}$ for both the ferromagnetic (FM) and AFM reference spin configurations to solve for $J_{nm}$ and $\beta_{nm}$. This yields

$$J_{nm} = \frac{1}{2}\left(D_{nm}^{(2),\text{FM}} + D_{nm}^{(2),\text{AFM}}\right), \qquad (5)$$

$$\beta_{nm} = \frac{1}{2}\frac{D_{nm}^{(2),\text{FM}} - D_{nm}^{(2),\text{AFM}}}{D_{nm}^{(2),\text{FM}} + D_{nm}^{(2),\text{AFM}}}. \qquad (6)$$

Our results for the nearest-neighbor constants of an infinite GT chain and a GT dimer are shown in Table I. We have also written in the table the values obtained experimentally in Ref. [16], where STM data were used to fit the spectrum of Eq. (1). Albeit our procedure gives somewhat higher values for both $J$ and $\beta$, the agreement between our parameter-

TABLE I. Nearest-neighbor $J$ and $\beta$ constants for a GT dimer, for an infinite GT chain obtained from Eqs. (5) and (6), and from the fit to STM experiments performed in Ref. [16].

|  | Dimer | Infinite chain | Experiment |
|---|---|---|---|
| $J$ (meV) | 17.7 | 19.75 | 18 |
| $\beta$ | 0.03 | 0.05 | 0.09 |

free first-principles approach and the experimental fittings of Ref. [16] is remarkable.

Our method allows us to determine the exchange constants between any two GT sites $n$ and $m$ in the chain. We have therefore computed the next-nearest-neighbor constants $J_{n\,n+2}$ and $\beta_{n\,n+2}$ and found that they are three to four orders of magnitude smaller than the nearest-neighbor parameters $J$ and $\beta$, providing compelling evidence of the accurate realization of open-ended and cyclic nearest-neighbor quantum AFM chains by the GT chains synthesized in Ref. [16].

### III. CONTROL OVER THE SINGLET-TRIPLET TRANSITION

Our first two proposals are based on the assumption that the exchange constant $J_{1N}$ can be modified by manipulating the distance between the ends of the GT chains. To achieve
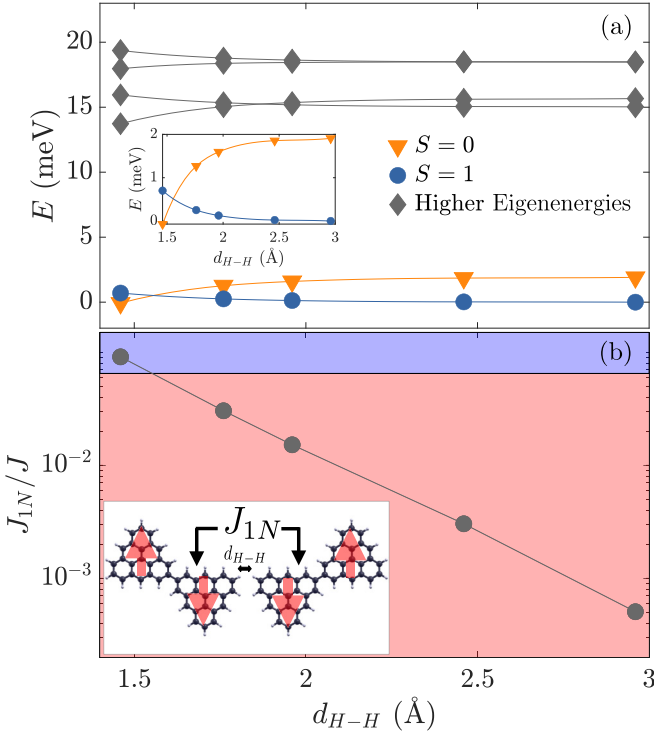
FIG. 3. (a) Lowest-lying energy states as a function of $d_{\text{H-H}}$ for a $N = 11$ chain. The plot shows that the singlet and triplet edge states lie inside the Haldane gap. Inset: Blowup of the energy axis to highlight the singlet-triplet energy splitting. (b) $J_{1N}/J$ as a function of $d_{\text{H-H}}$. The horizontal line identifies the critical $J_{1N}$ separating the regions where the ground state is a triplet (pink) or a singlet (violet). Inset: Sketch of the horseshoe chain end where the distance $d_{\text{H-H}}$ is defined.
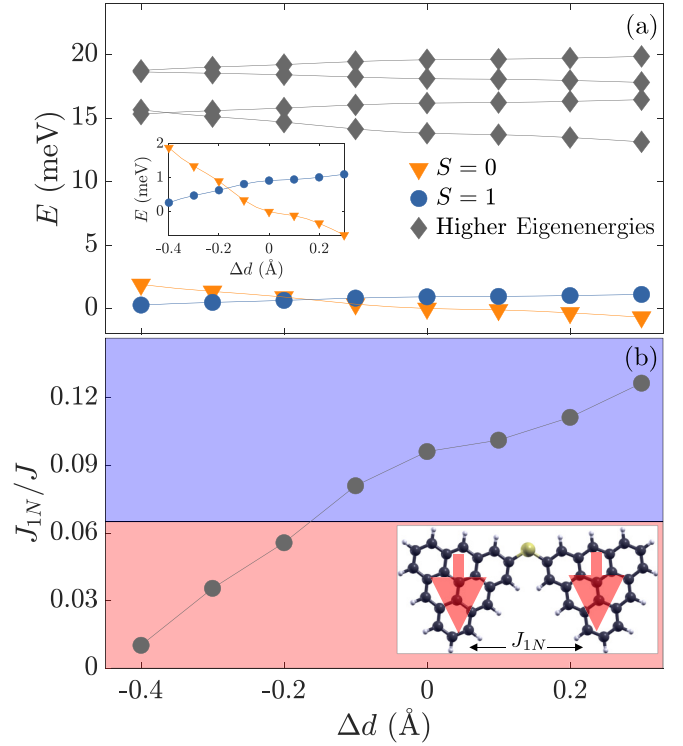
FIG. 4. (a) and (b) Same as in Fig. 3, but where the horseshoe chain is linked by a sulfur atom.

realistic values for $J_{1N}^c$, we select horseshoelike chains of lengths in the range $N \in [7, 15]$. We have chosen to demonstrate numerically our proposals for a $N = 11$ chain, because in this case the singlet-triplet splitting is of the order of a few meV, so that it should be measurable by spectroscopic STM methods [16,19,20]. We have hence checked whether we can increase $J_{1N}$ by bringing the ends of the horseshoe chain sufficiently close. We have found that $J_{1N} \sim J_{1N}^c$ requires forces of the order of 100 meV/Å, which may be realized in STM experiments [16,20].

Within the first proposal, we assume that the distance $d_{\text{H-H}}$ between the closest hydrogen atoms at the two chain ends can be changed in a controlled way [see the inset in Fig. 3(b) for a graphical definition of $d_{\text{H-H}}$]. We have therefore computed $J_{1N}$ as a function of $d_{\text{H-H}}$. As expected, $J_{1N}$ increases exponentially with decreasing $d_{\text{H-H}}$. Consequently, the energy difference between the triplet and singlet states decreases, and as seen in Fig. 3(b), the $N = 11$ horseshoe GT chain experiences a singlet-triplet level crossing at $d_{\text{H-H}} \sim 1.6$ Å. The force needed to bring the two dimers in Fig. 3 to $d_{\text{H-H}} \sim 1.6$ Å is about 0.1 eV/Å. To achieve a splitting $\Delta E_{\text{ST}}$ of about 1 meV, we need to reduce the distance further to $d_{\text{H-H}} \sim 1.45$ Å, which requires the application of higher forces of about 0.5 eV/Å. This is a lower bound to the full required force that does not take into account the tensile stress caused by the deformation inside the full horseshoe chain. However, we expect that this contribution should not dominate for chains as long as $N = 11$.

Linking atoms such as nitrogen, sulfur, phosphorous, or oxygen to metallic surfaces or to graphene edges is routinely done in areas such as molecular electronics [28].
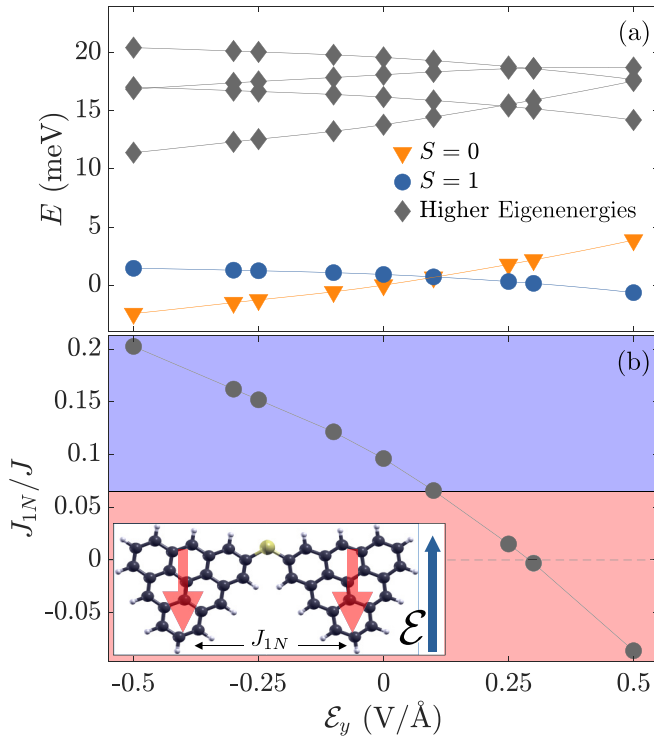
FIG. 5. (a) and (b) Same as in Fig. 3, but where in addition to a linking sulfur atom, an electric field $\mathcal{E}$ is being applied along the chain main axis.

Our second proposal is similar to the first one, but now both closest hydrogen atoms at the GT ends are replaced by a single sulfur atom that links the ends of the chain as illustrated in the inset of Fig. 4(b). Our DFT simulations show that the sulfur atom does not change the magnetic moment of the two adjacent GTs. We then compute $J_{1N}$ as a function of the distance $\Delta d$ relative to the equilibrium distance of the two edges. Our results, depicted in Fig. 4(b), demonstrate that the singlet-triplet level crossing can be triggered by closing the structure by about 0.3 Å. We find forces now of order 0.7 eV/Å for $\Delta d \sim -0.4$ Å, where $\Delta E_{ST} \sim 1.5$ meV.

The third proposal is based on the observation that the sulfur atom introduces an electric dipole at the chain weak link that renders $J_{1N}$ susceptible to an external electric field $\mathcal{E}$. Our first-principles simulations confirm that this is the case, $\mathcal{E}$ being most effective when pointing along the symmetry axis of the horseshoe-shaped GT chain. We plot in Fig. 5 the energies of the singlet and triplet states, as well as the exchange constant $J_{1N}$ as a function of $\mathcal{E}_y$. Indeed, we find that there is a level crossing from singlet to triplet at about $\mathcal{E}_y \sim 0.1$ V/Å.

We find a threshold coupling $J_{1N}^c \sim 0.06 J$ that agrees well with the estimates from our exact diagonalization studies for $N = 11$ and $\beta = 0.05$, shown in Fig. 2(a). Our numerical study provides strong evidence that the single-triplet transition can be sensitively controlled by an electric field.

To clarify the physical origin of the electric-field-based mechanism, we have first checked that the spin of each GT remains equal to 1 and that the exchange constant $J$ between the GTs in the chain changes only by about 1–2 meV even for the largest simulated fields. We have also checked that the electric field does not affect the chain geometry even around the sulfur atom. We have then investigated the redistribution of atomic Mulliken charges at the terminating GTs when the sulfur atom is present at the junction. We have then found that the combined influence of the sulfur atom and the electric field induces an internal dipole in those GTs. Further calculations in the Supplemental Material [21] show that $J_{1N}$ is linearly proportional not only to the external electric field but also to the electric dipole moment at the junction.

## IV. CONCLUSIONS

We have demonstrated that GT chains are faithful realizations of the nearest-neighbor spin-1 AFM chain by combining spin-model simulations with first-principles calculations. We have advanced three proposals for experiments that may trigger and control the singlet-triplet transition of odd-numbered chains, thus opening the door for their future use as quantum devices. Our calculations indicate that the application of an external electric field is particularly feasible.

[1] E. Ising, Beitrag zur theorie des ferromagnetismus, Z. Phys. **31**, 253 (1925).

[2] W. Heisenberg, Zur theorie des ferromagnetismus, Z. Phys. **49**, 619 (1928).

[3] F. D. M. Haldane, Continuum dynamics of the 1-D Heisenberg antiferromagnet: Identification with the O(3) nonlinear sigma model, Phys. Lett. A **93**, 464 (1983).

[4] A. Y. Kitaev, Fault-tolerant quantum computation by anyons, Ann. Phys. (Amsterdam) **303**, 2 (2003).

[5] T.-C. Wei, I. Affleck, and R. Raussendorf, Two-dimensional Affleck-Kennedy-Lieb-Tasaki state on the honeycomb lattice is a universal resource for quantum computation, Phys. Rev. A **86**, 032328 (2012).

[6] A. Kitaev, Anyons in an exactly solved model and beyond, Ann. Phys. (Amsterdam) **321**, 2 (2006).

[7] I. Affleck, T. Kennedy, E. H. Lieb, and H. Tasaki, Rigorous Results on Valence-Bond Ground States in Antiferromagnets, Phys. Rev. Lett. **59**, 799 (1987).

[8] A. Auerbach, *Interacting Electrons and Quantum Magnetism* (Springer, New York, 2012).

[9] T. Kennedy, Exact diagonalisations of open spin-1 chains, J. Phys.: Condens. Matter **2**, 5737 (1990).

[10] S. R. White and D. A. Huse, Numerical renormalization-group study of low-lying eigenstates of the antiferromagnetic $S = 1$ Heisenberg chain, Phys. Rev. B **48**, 3844 (1993).

[11] M. D. Shulman, O. E. Dial, S. P. Harvey, H. Bluhm, V. Umansky, and A. Yacoby, Demonstration of entanglement of electrostatically coupled singlet-triplet qubits, Science **336**, 202 (2012).

[12] B. Jaworowski, N. Rogers, M. Grabowski, and P. Hawrylak, Macroscopic singlet-triplet qubit in synthetic spin-one chain in semiconductor nanowires, Sci. Rep. **7**, 5529 (2017).

[13] P. Sompet, S. Hirthe, D. Bourgund, T. Chalopin, J. Bibo, J. Koepsell, P. Bojović, R. Verresen, F. Pollmann, G. Salomon, C. Gross, T. A. Hilker, and I. Bloch, Realizing the symmetry-protected Haldane phase in Fermi–Hubbard ladders, Nature (London) **606**, 484 (2022).

[14] J. Su, M. Telychko, S. Song, and J. Lu, Triangulenes: From precursor design to on-surface synthesis and characterization, Angew. Chem. Int. Ed. **59**, 7658 (2020).

[15] T. Wang, A. Berdonces-Layunta, N. Friedrich, M. Vilas-Varela, J. P. Calupitan, J. I. Pascual, D. Peña, D. Casanova, M. Corso, and D. G. de Oteyza, Aza-triangulene: On-surface synthesis and electronic and magnetic properties, J. Am. Chem. Soc. **144**, 4522 (2022).

[16] S. Mishra, G. Catarina, F.-P. Wu, R. Ortiz, D. Jacob, K. Eimre, J. Ma, C. Pignedoli, X. Feng, P. Ruffieux, J. Fernández-Rossier, and R. Fasel, Observation of fractional edge excitations in nanographene spin chains, Nature (London) **598**, 287 (2021).

[17] E. H. Lieb, Two Theorems on the Hubbard Model, Phys. Rev. Lett. **62**, 1201 (1989).

[18] J. Fernández-Rossier and J. J. Palacios, Magnetism in Graphene Nanoislands, Phys. Rev. Lett. **99**, 177204 (2007).

[19] S. Wang, L. Talirz, C. A. Pignedoli, X. Feng, K. Mullen, R. Fasel, and P. Ruffieux, Giant edge state splitting at atomically precise graphene zigzag edges, Nat. Commun. **7**, 11507 (2016).

[20] J. Lawrence, P. Brandimarte, A. Berdonces-Layunta, A. Mohammed, Mohammed S. G. Grewal, C. C. Leon, D. Sańchez-Portal, and D. G. de Oteyza, Probing the magnetism of topological end states in 5-armchair graphene nanoribbons, ACS Nano **14**, 4499 (2020).

[21] See Supplemental Material at http://link.aps.org/supplemental/10.1103/PhysRevB.107.035432 for further calculations.

[22] J. M. Soler, E. Artacho, J. D. Gale, A. García, J. Junquera, P. Ordejón, and D. Sánchez-Portal, The SIESTA method for *ab initio* order-*N* materials simulation, J. Phys.: Condens. Matter **14**, 2745 (2002).

[23] J. P. Perdew, K. Burke, and M. Ernzerhof, Generalized Gradient Approximation Made Simple, Phys. Rev. Lett. **77**, 3865 (1996).

[24] L. Oroszlány, J. Ferrer, A. Deák, L. Udvardi, and L. Szunyogh, Exchange interactions from a nonorthogonal basis set: From bulk ferromagnets to the magnetism in low-dimensional graphene systems, Phys. Rev. B **99**, 224412 (2019).

[25] A. Liechtenstein, M. Katsnelson, V. Antropov, and V. Gubanov, Local spin density functional approach to the theory of exchange interactions in ferromagnetic metals and alloys, J. Magn. Magn. Mater. **67**, 65 (1987).

[26] M. I. Katsnelson and A. I. Lichtenstein, First-principles calculations of magnetic interactions in correlated systems, Phys. Rev. B **61**, 8906 (2000).

[27] L. Udvardi, L. Szunyogh, K. Palotás, and P. Weinberger, First-principles relativistic study of spin waves in thin magnetic films, Phys. Rev. B **68**, 104436 (2003).

[28] J. C. Cuevas and E. Scheer, *Molecular Electronics* (World Scientific, Singapore, 2017).